The Effect of Observation Errors on the Assessment of Insurance Losses due to Seismic Activity

By: S Pretorius [a]

a: Department of Insurance and Actuarial Science, University of Pretoria, Private Bag X20, Pretoria, 0028, South Africa

Abstract

The paper discusses the development of several procedures for estimating parameters of statistical models, by making allowances for the errors inherent in observed data and applying this to a data set describing the South African insurance landscape. The classical assumption that the real observation is a sum of two random variables, namely the actual (true) value of the observed variable and observational error, is considered. Most often the error is assumed to be distributed as Gaussian noise; however, other distributions for the error function may sometimes offer better approximations. The paper considers the Laplacian distribution as an additional option. The approach is applied, for both assumptions as well as for other well-known methodologies, to estimate parameters of the frequency-magnitude Gutenberg-Richer relation, which describes the distribution of different sizes of earthquakes. The implications of the newly derived estimation procedures for the insurance industry are also discussed. This pertains specifically to the estimation procedures serving as a means to improve the hazard at risk for short term property reinsurance caused by earthquakes. A discussion of the probabilistic seismic risk assessment methodology and an application to the South African insurance landscape underpins the above investigation.

Keywords:

Observation errors, parameter estimates, reinsurance, earthquake magnitudes, catastrophe insurance, probabilistic seismic risk analysis

1. Introduction

Increasing global urbanisation means that the potential impact of a catastrophic event, such as an earthquake, is increasing. To this end, insurers are taking a more comprehensive view of managing and understanding risk. This means that catastrophe models are becoming more sophisticated and the importance of accurate input data is becoming increasingly important (Grossi and Zoback, 2009). By increasing the accuracy of the input parameters for earthquake recurrence, it is predicted that ultimate insurance loss forecasts will be more accurate and more prudent. This paper will mainly investigate ways of refining the input parameters and their possible effects on insurance losses.

2. Earthquake magnitude and uncertainty

2.1 The Gutenberg-Richter relation

The Gutenberg-Richter relation (Gutenberg and Richter, 1954) describes the relationship between the number of earthquakes and their associated magnitudes for a variety of tectonic settings. The importance of the Gutenberg-Richter relation and its applications to a range of industries that are concerned with earthquake recurrence forecasting, for example, engineering, insurance and reinsurance companies as well as disaster management, further emphasises the importance of accurate forecasting. The occurrence of majorly catastrophic earthquakes (i.e. where more than 50 000 deaths occur) are few and far between, see Appendix 1. The increasing population density in earthquake prone areas is cause for concern that the destructive power of future earthquakes, particularly near heavily populated areas, will increase greatly (Grossi *et al*., 2005).

The relation is given by:

$$\log(N) = a - bM \tag{2.1.1}$$

Where N is the number of events with magnitude M , and *a* and *b* are coefficients (Gutenberg and Richter, 1954).

The applicability of the relation in a wide range of scenarios ensures that it is of significant scientific importance in the field of earthquake occurrence. It can be used to describe both induced and tectonic seismicity, over different time scales and over a large range of earthquake magnitudes (Kijko and Smit, 2012). To understand the relation, we must first look at measures of earthquake magnitude.

2.2 Measures of earthquake magnitude and intensity

Magnitude is the most well-known measure of the “size” of an earthquake and was introduced by Charles Richter and Beno Gutenberg during the 1930s. There are several different types of magnitude which are based on different characteristics of earthquake seismic waves, as measured by seismographs (Werner and Sornette, 2008).

Of particular interest is the uncertainty that arises for individual magnitude observations. Several contributing factors add to the errors that are inherent in an observed magnitude. These factors include, but are not limited to, the effects of discretization of media and equations, the measurement precision of seismometers, the assumed velocity and attenuation models of the Earth, the resolution of the inversion algorithm, and, most particularly, the definition of an earthquake event (Werner and Sornette, 2008).

The magnitude of an earthquake is never accurately known. Unit accuracy ranges from 0.1 units for recent magnitudes, to 0.25 units for older magnitudes and up to 0.6 units for paleoseismic earthquakes (Kijko, 1988). Paleoseismic earthquakes refer to those earthquakes that are recovered from historical records and were not directly observed with the help of modern instruments. The unit accuracy clearly indicates that modern earthquake catalogues contain fewer errors than paleoseismic studies, but the additional factors described above still mean that some uncertainty is still present (Werner & Sornette, 2008).

Additionally, for the purposes of assessing losses that can be attributed to seismic events, we need to measure the strength of a seismic event at a given site in terms of the resultant structural damage to buildings. A well-known measure is the Modified Mercalli (MM) intensity scale. Full details of each intensity measure are outlined in Appendix 2. Since the scale is, for the most part, subjective, further uncertainty persists, especially where eye-witness accounts make up the majority of the body of evidence to determine the magnitude of a particular event. (Davies and Kijko, 2003)

2.3 Estimating the Gutenberg-Richter parameters

Estimation of the parameters of the Gutenberg-Richter relation is of particular importance and an extensive body of work exists on the subject. The *a* parameter is a measure of the level, or rate, of seismicity and the *b* value describes the proportion of seismic events with different magnitudes or the relationship between the number of small and large seismic events (Kijko and Smit, 2012; Bengoubou-Valérius and Gilbert, 2013). For global seismicity, the *b* value is approximately 1 (Kagan, 1999), but has been shown to vary significantly between regions (Wiemer and Benoit, 1996; Ayele and Kulhánek, 1997; Wiemer *et al*., 1998; Gerstenberger *et al*., 2001; Schorlemmer *et al*., 2003).

Prior to 1964, the parameters of the Gutenberg-Richter relation (2.1.1) were estimated by the traditional least squares method. This method is based on the principle of least squares, which minimises the sum of the squared deviations from the fitted line (Bain and Engelhardt, 1992*).* Consequent investigations indicate that the least squares technique was by far the most inaccurate means of estimating the *b*-value of the Gutenberg-Richter relation (Marzocchi and Sandri, 2006). Additionally, the least squares method of estimation does not have any statistical foundation for this particular case (Page, 1968; Bender and Bannert, 1983).

In general, any uncertainties can be divided into two main categories, namely aleatory and epistemic uncertainty. Aleatory uncertainties "*are those uncertainties that for all practical purposes cannot be known in detail or cannot be reduced"* (Budnitz, *et al.,* 1997), this is also referred to as systematic uncertainty (Ku, 1969). Epistemic uncertainties, however, are those uncertainties that arise from a "lack of knowledge", for the present (Budnitz, *et al.*, 1997). Therefore, epistemic uncertainties can be reduced by more adequate models or by better measurement techniques. This type of uncertainty is also referred to as random error (Ku, 1969) and is the main type of uncertainty that affects magnitude observations (Kijko, 1988).

In 1964, two Japanese seismologists, K. Aki and T. Utsu, working independently, proposed the new formula: (Aki, 1964; Utsu 1964)

$$\hat{b} = \frac{\log_{10} e}{\bar{m} - m_{\min}} \tag{2.3.1}$$

which is both the moment and maximum likelihood estimator of the *b*-value. In (2.3.1), $m_{\min}$ denotes the level of completeness of the catalogue, or the smallest observed magnitude within the catalogue.

From the maximum likelihood estimator above we can infer that the probability distribution function of earthquake magnitude is:

$$f_M(m) = \frac{\beta}{e^{-\beta m_{\min}} - e^{-\beta m_{\max}}} e^{-\beta m} \qquad m_{\min} \le m \le m_{\max} \tag{2.3.2}$$

and that the parameters of the Gutenberg-Richter relation are related to the above by:

$$a = \log \lambda + b m_{\min} \tag{2.3.3}$$

$$b = \frac{\beta}{\log(e)} \tag{2.3.4}$$

Where λ is the mean activity rate which is defined as the number of earthquakes in the catalogue that exceed $m_{\min}$ divided by the time interval under investigation. (Kijko, 2011)

It is notable that the Aki-Utsu estimator (2.3.1) does not include magnitude uncertainty. The effects of magnitude uncertainties in the data used to estimate the *b*-value and consequently seismic hazard and risk remained largely unexplored for some time. However, this oversight has since been corrected by several others (Shi and Bolt, 1982; Tinti and Mulargia, 1985; Kijko, 1988; Rhoades, 1996; Dowrick and Rhoades 2000; and Marzocchi and Sandri, 2003). Furthermore the Aki-Utsu estimator does not include the upper bound for the magnitudes, $m_{\max}$. An estimator that includes this upper bound is the maximum likelihood estimator for the double truncated exponential distribution:

$$\frac{1}{\hat{\beta}} - \overline{m} + \frac{\left(M_{\max} e^{\hat{\beta} M_{\min}} - M_{\min} e^{\hat{\beta} M_{\max}} \right)}{\left(e^{\hat{\beta} M_{\min}} - e^{\hat{\beta} M_{\max}} \right)} = 0 \tag{2.3.5}$$

The first mention of potential bias in the *a* and *b* parameters of Gutenberg-Richter relation (2.1.1) due to magnitude uncertainty was made by Tinti and Mulargia (1985). In this particular paper, the authors propose an improved estimate for parameters *a* and *b*, by treating the observed magnitudes as random variables with normally distributed observational errors. The findings of this paper are reiterated by Marzocchi and Sandri (2003). The studies show that magnitude errors do not cause significant bias in the estimation of the *b* parameter if the same degree of earthquake magnitude uncertainty (standard deviation) applies to all the magnitudes (Tinti and Mulargia, 1985).

Research by Werner and Sornette (2008) found that, in case of large magnitude uncertainties, the double-exponential (Laplace) distribution describes the observation errors significantly better than a Gaussian distribution. The use of the Laplacian (or double exponential) distribution, as opposed to the traditionally assumed Gaussian distribution under-estimates the occurrence of large error outliers. Consequently, this assumption leads to more conservative assumptions regarding the influence of errors. Intuitively, this approach makes sense, since errors in modern earthquake catalogues are not large, but their compounding effect can be significant.

Measurement uncertainty has been reduced over time due to the introduction of higher-quality instrumentation (Rhoades, 1996), which would again lead to the fact that uncertainties in magnitude

determination are not the same for whole earthquake catalogues that stretch over considerable periods of time. Some studies have attempted to provide improved estimates for the *b*-parameter by taking uncertainties into account (Rhoades, 1996, Kijko, 1988). It is notable, however, that the moment magnitude is believed to be the most stable with uncertainties around 0.1 (Werner and Sornette, 2008; Kijko, 1988).

The approach by Rhoades (1996) proposes a probability distribution of magnitudes of earthquakes in a catalogue as the sum of a uniform random variable and a normal random variable with mean $y-\sigma^2\beta$ and variance σ^2. Thus the paper proposes an adjustment to each observed magnitude of ($-\sigma^2\beta$), although it is shown that often this provides an over-correction to the bias (Rhoades, 1996). Kijko's (1988) approach is based on the assumption that the observed magnitudes are each from a uniformly distributed interval and proceeds to calculate a maximum likelihood estimate.

The latter two approaches succeed in calculating more accurate estimates for the *b*-parameter, however, the procedures are either too extensive to be used in practice and are too dependent on the quality of the data. There is an apparent need for an approach that will be less onerous to implement and possibly lead to equally accurate, if not more accurate, assumptions of the *b*-value.

2.4 Estimating the b value

There are many ways in which observation errors can be taken into account. A method well-described by Marzocchi and Sandri (2003) involves the classical assumption that the real observation $\tilde{Y}$ is a sum of two random variables, namely, the actual observation Y and some error ε, is considered. This paper (Marzocchi and Sandri, 2003) specifically discusses observation errors for the Gutenberg-Richter relation for earthquake magnitude predictions and its effect on the b-value of this relation. Better estimates are then derived for the parameters of the model by deriving a distribution for the real observations and obtaining a maximum likelihood estimate from the distribution. Most often the error is assumed to follow a Gaussian distribution with a mean of zero and some variance relating to the errors. This leads to the estimate for the *b* value of:

$$\left(\frac{1}{\hat{\beta}}-\bar{m}+\frac{\left(M_{\max}e^{\hat{\beta}M_{\min}}-M_{\min}e^{\hat{\beta}M_{\max}}\right)}{\left(e^{\hat{\beta}M_{\min}}-e^{\hat{\beta}M_{\max}}\right)}\right)+$$
$$\left(\hat{\beta}\sigma^2+\frac{1}{n}\sum_{i=1}^{n}\frac{\sqrt{2}\sigma\left(e^{-\frac{\left(M_{\max}+\hat{\beta}\sigma^2-m_i\right)^2}{2\sigma^2}}-e^{-\frac{\left(M_{\min}+\hat{\beta}\sigma^2-m_i\right)^2}{2\sigma^2}}\right)}{\sqrt{\pi}\left[erf\left(\frac{M_{\max}+\hat{\beta}\sigma^2-m_i}{\sqrt{2}\sigma}\right)-erf\left(\frac{M_{\min}+\hat{\beta}\sigma^2-m_i}{\sqrt{2}\sigma}\right)\right]}\right)=0$$

(2.4.1)

where $\bar{m}$ is the sample mean of the observed magnitudes. The expression in the first set of brackets corresponds with estimator (2.3.6) and the latter part indicates the adjustment in the estimator for the magnitude uncertainties, taking the level of completeness and maximum possible earthquake

into account. If the standard deviation of the errors tends to zero, the estimator is exactly as outlined in (2.3.6).

Research by Werner and Sornette (2008) found that, in case of large magnitude uncertainties, the double-exponential, or Laplace, distribution describes the observation errors significantly better than a Gaussian distribution. If we apply the traditional method outlined above, but change the assumption of the distribution of the errors, to one where the errors follow a double exponential distribution with a zero mean, we arrive at the following estimate for the *b* value:

$$\left(\frac{1}{\hat{\beta}}-\overline{m}+\frac{\left(M_{\max}e^{\hat{\beta}M_{\min}}-M_{\min}e^{\hat{\beta}M_{\max}}\right)}{\left(e^{\hat{\beta}M_{\min}}-e^{\hat{\beta}M_{\max}}\right)}\right)+$$
$$+\left\{\frac{2\nu_c^2\beta}{\nu_c^2\beta-1}+\frac{1}{n}\prod_{i=0}^{n}\left\{\frac{\left(\nu_c+\left(m_i-M_{\min}\right)\left(\beta\nu_c-1\right)\right)\left[e^{\frac{\left(m_i-M_{\min}\right)\left(\beta\nu_c-1\right)}{\nu_c}}\right]+\left(\nu_c+\left(m_i-M_{\max}\right)\left(\beta\nu_c+1\right)\right)\left[e^{\frac{\left(M_{\max}-m_i\right)\left(\beta\nu_c+1\right)}{\nu_c}}\right]}{\left(\beta\nu_c+1\right)\left[e^{\frac{\left(M_{\max}-m_i\right)\left(\beta\nu_c+1\right)}{\nu_c}}\right]+\left(\beta\nu_c-1\right)\left[e^{\frac{\left(m_i-M_{\min}\right)\left(\beta\nu_c-1\right)}{\nu_c}}\right]}\right\}\right\}$$
$$=0$$

(2.4.2)

Where $\overline{m}$ is the sample mean of the observed magnitudes. Once again, the expression in the first set of brackets corresponds with that of estimator (2.3.6) and the latter part indicates the adjustment in the estimator for the magnitude uncertainties, taking the level of completeness and maximum possible earthquake into account.

2.5 Estimating the a-value

As previously discussed (equation 2.2.3), the *a* value depends on the mean activity rate of the catalogue, the minimum magnitude under investigation and the *b* value. Thus any uncertainty incorporated in the estimate of the *b* value will be translated into the estimate of the *a* value.

3. Earthquakes and the Insurance Industry

3.1 Background

Traditionally, reinsurers supply indemnity contracts against unforeseen or extraordinary losses to insurers. In terms of earthquakes, reinsurers usually write catastrophe excess of loss reinsurance. This is a non-proportional type of reinsurance that protects the reinsured against potential aggregation or accumulation of losses that might arise as a result of natural perils. For an excess of loss reinsurance product the insured covers all losses up to, and including, a fixed monetary amount, the reinsurer pays amounts in excess of this figure up to a further identified amount or limit of the

layer. A reinsured may purchase several "layers" of excess of loss reinsurance from different reinsurers. (Paine, 2004)

In order to determine the effects that an earthquake can have on a particular area, we need to determine the adverse consequences of a seismic event. Generally, it is also useful to estimate the probabilities associated with these consequences. Catastrophe models that do just this built exclusively for the insurance industry first emerged in the 1980s. For earthquake hazard, the models were mainly focused on risks in the United States (Grossi and Zoback, 2009). Natural hazards are problematic for insurers and reinsurers since they involve potentially high losses that are extremely uncertain (Grossi *et al.*, 2005).

Actuarial approaches to managing risk is useful for pricing different types of risk, but fails when applied to low probability, high severity events like earthquakes (Grossi and Zoback, 2009). For these situations, modelling is a much more effective solution.

When modelling catastrophes, there are three elements to consider: the most likely locations of the future events, their frequency of occurrence and their severity (Grossi *et al.*, 2005). By taking these elements into account, insurers can forecast future losses and attach a probability of occurrence to the losses. By multiplying the potential loss of an event by the probability of occurrence of said event, reinsurers can price products accurately and can also limit their exposure in areas where substantial, regular losses are forecast (Paine, 2004). Whilst the potential losses can be estimated for natural disasters of a given size, the probability of occurrence is of importance. While the potential losses can be estimated for natural disasters of a given size, the probability of occurrence is of importance since it is usually more difficult to calculate.

A very basic catastrophe model for the purposes of seismic risk analysis would be constructed as follows:

> The historical earthquake data will be analysed to derive an occurrence model. Thereafter, the occurrence model will be used to generate a stochastic event set with the expected annual rate of occurrence. The site intensity will then be calculated, taking cognisance of the distance from the site to the epicentre, the magnitude of the event and the soil conditions. The site intensity is then transformed into damage ratios depending on construction classes. (Liechti, *et al*., 2000)

By improving the accuracy of a catastrophe model, or at the very least the accuracy of the elements that make up the model, reinsurers will be able to construct more accurate catastrophe models, which will ultimately lead to better financial preparedness for catastrophic events. An increase in the accuracy of the *b* parameter will most probably lead to an increase in the level of accuracy.

3.2 Probabilistic Seismic Risk Analysis

In order to assess the impact of changes in the Gutenberg-Richter relation's parameters we need to use a seismic risk model to assess the possible losses for different scenarios. To this end, a probabilistic seismic risk assessment (PSRA) will be conducted for different parameter values.

Deterministic studies are used frequently in the insurance industry and are also known as the probable maximum loss calculation. The deterministic approach only considers the worst case scenario earthquake. The probabilistic approach used here and outlined by Davies and Kijko (2003) not only includes the most sever seismic event, but looks at the range of events that are likely to occur over a particular time period. For insurance purposes, a time interval of one year is sufficient since most cover is reviewed annually.

It must be noted that the deterministic and probabilistic approaches should be considered together since this considers the problem of seismic risk holistically. It is, however, difficult to classify models in this area of investigation as purely deterministic since they will most likely contain some probabilistic elements. (Davies and Kijko, 2003) Probabilistic models are used extensively to estimate possible losses in seismic risk analysis (Cornell, 1968; Shah and Dong, 1991; Schmid and Schaad, 1995). One of the main components of seismic risk analysis, attenuation functions, is complemented by earthquake occurrence models. Of the earthquake occurrence models in use, most are based on the Gutenberg-Richer relation (Liechti *et al*., 2000).

What follows is a summary of the probabilistic seismic risk analysis procedure described by Davies and Kijko (2003).

In order to assess the seismic risk for a particular area, we first need to conduct a probabilistic seismic hazard assessment (PSHA). According to Davies and Kijko (2003) seismic hazard is:

> "…the probability of occurrence, within a specified period of time, of a seismic event that could damage buildings or objects."

To connect hazard and risk, we need some kind of connection between seismic parameters and damages and losses. The PSRA under discussion suggests the use of the work of Whitman *et al* (1973). The damage probability matrix (DPM) divides the extent of damage into different states (Table 3.2.1) and by a range of damage factors or damage expressed as a percentage of the total replacement value of the structure. A typical DPM is represented in Table 3.2.2.

Additionally, the assessment needs to measure the strength of a seismic event at a given site in terms of the resultant structural damage to buildings, for which we use the MM intensity scale as discussed in section 2 and outlined in appendix 2.

Due to the nature of the South African seismic landscape, which has not suffered much damage in recent history, the data required to compile a complete vulnerability assessment is somewhat limited. There are several ways in which damage curves of particular types of buildings can be established, some procedures that can be considered are statistical analysis, subjective expert opinion or detailed analytical tools (Kijko and Smit, 2012). The most popular methodology applied by South African agencies is the ATC-13 methodology. ATC-13 is a seismic risk study that was conducted by the Applied Technology Council in 1985. The Earthquake Damage Evaluation Data for California report was prepared as a result thereof (ATC-13, 1985). This is also the report that will be used for different building classes in this study.

The results that are produced by conducting the PSRA produces 12 vulnerability curves (the expected damage to a structure for a given intensity) for 12 different classes of buildings, where the DPM matrices are provided by the ATC-13 (1985).

Table 3.2.1

Description of damage factors

Damage Factor	Damage Factor Name	Description
1	None	No damage
2	Slight	Limited localised minor damage not requiring repair
3	Light	Significant localised damage of some components generally not requiring repair
4	Moderate	Significant localised damage of many components warranting repair
5	Heavy	Extensive damage requiring major repairs
6	Major	Widespread damage that may result in the facility being razed
7	Destroyed	Total destruction of the majority of the facility

(Source: Whitman *et al*, 1973)

Table 3.2.2

Example of a DPM for a specific building class

Damage Factor	Damage Factor Range (%)	Central Damage Factor (%)	Probability of damage (%) by MM intensity and damage state				
			VI	*VII*	*VIII*	*IX*	*X*
1	0	0.0	95.0	49.0	30.0	14.0	3.0
2	0-1	0.5	3.0	38.0	40.0	30.0	10.0
3	1-10	5.0	1.5	8.0	16.0	24.0	30.0
4	10-30	20.0	0.4	2.0	8.0	16.0	26.0
5	30-60	45.0	0.1	1.5	3.0	10.0	18.0
6	60-100	80.0	0.0	1.0	2.0	4.0	10.0
7	100	100.0	0.0	0.5	1.0	2.0	3.0

(Source: Panel on Earthquake Loss Estimation Methodology, 1989: 82)

The 12 building class types used in the PSRA for the purposes of this study) are defined in Table 3.2.3. Four of the building classes, namely:

- Unreinforced masonry, with load bearing wall, low rise (Class #3),
- Reinforced concrete shear wall without moment resisting frame, high rise (Class #7),
- Reinforced concrete shear wall without moment resisting frame, medium rise (Class #8), and
- Reinforced concrete shear wall without moment resisting frame, high rise (Class #9)

which represent the most prevalent structures in South Africa. Some rough estimates imply that these four classes represent over 80% of all South African urban buildings (Davies and Kijko, 2003). Figures 3.2.1 to 3.2.3 represent examples of these buildings.

"The results of the PSHA are used to estimate seismic risk by translating probabilistic estimates of ground motion into damage via ground-motion-damage relationships."

Earthquakes cause the ground to vibrate, meaning that any motion will not be constant. In order to assess the movement of the ground we examine the peak ground acceleration (PGA), *a'*, which is the maximum value of the acceleration recorded at a particular site during an event.

The PGA is characterised by the following attenuation function:

$$\ln(a') = c_1 + c_2 M + c_3 R + c_4 \ln(R) + \varepsilon$$

Where c_1, c_2, c_3, c_4 are empirical constants, M is the Richter magnitude of the earthquake, R is the distance from the epicentre and ε is a random error, assumed to follow a Gaussian distribution with a mean of zero and a standard deviation of $\sigma_{a'}$. (Boore and Joyner, 1982; Ambraseys, 1995).

Table 3.2.3

Description of building classes

Description of Class of Building	**Ref. No.**
Wood Frame, Low rise	1
Light Metal, Low Rise	2
Unreinforced Masonry, Bearing Wall, Low Rise	3
Unreinforced Masonry, Load Bearing, Frame, Low Rise	4
Unreinforced Masonry, Load Bearing, Frame, Medium Rise	5
Reinforced Concrete Shear Wall with Moment-Resisting Frame, Medium Rise	6
Reinforced Concrete Shear Wall with Moment-Resisting Frame, High Rise	7
Reinforced Concrete Shear Wall without Moment-Resisting Frame, Medium Rise	8
Reinforced Concrete Shear Wall without Moment-Resisting Frame, High Rise	9
Braced Steel Frame, Low Rise	10
Precast Concrete, Low Rise	11
Long Span, Low Rise	12

(Source: ATC-13, 1985)

Figure 3.2.1

Building Class 3: Unreinforced masonry, with load bearing wall, low rise

Source: EMS, (1998)

Figure 3.2.2

Building Class 7: Reinforced concrete shear wall, with moment resisting frame, high rise

(Source: panoramio.com, 2008)

Figure 3.2.3

Building Class 8: Reinforced concrete shear wall, without moment resisting frame, medium rise

(Source: EMS, 1998)

Figure 3.2.4

Building Class 9: Reinforced concrete shear wall, without moment resisting frame, high rise

(Source: EMS, 1998)

According to Davies and Kijko (2003):

For the purposes of the PSRA we define seismic hazard, $H(a';T)$, as "the probability that a certain level of ground shaking characterised by PGA, will be exceeded at least once within the specified time interval, T" (Davies and Kijko 2003).

$$H(a';T) = 1 - F_{A'}^{MAX}(a';T)$$

where $F_{A'}^{MAX}(a';T)$ is the cumulative distribution function of the PGA in the specified time interval.

There is no direct link between PGA and seismic risk, so the assessment model links PGA with damage via MM intensity as follows:

$$p_D(d;T) = \int_{d}^{d_{\max}} \int_{i_{\min}}^{i_{\max}} \int_{a_{\min}}^{a_{\max}} f_D(\tilde{d} \mid i)\, f_I(i \mid a')\, f_{A'}^{MAX}(a';T)\, \mathrm{d}a'\, \mathrm{d}i\, \mathrm{d}\tilde{d}$$

With $f_I(i \mid a')$ being the conditional probability distribution function for the MM intensity, I, given the PGA and $f_D(d \mid i)$ being the conditional probability distribution function for the damage, D, for a given MM intensity.

The bounds for the integrals were determined. The minimum PGA should be the PGA above which damage to infrastructure is likely to result, also termed the PGA of engineering interest. This is usually $0.05g$, where g is the acceleration due to gravity. The maximum PGA is the maximum possible at the site being investigated. The intensity is determined as the scales for the MM intensity which range from IV to XII, since, for scales less than IV, no damage results. Finally the maximum possible damage is 100% of the total replacement value of the building.

In terms of an insurance application, we are interested in the expected damage over a particular period of time:

$$\begin{aligned} E\left[D(t)\right] &= \int_{d_{\min}}^{d_{\max}} \int_{i_{\min}}^{i_{\max}} \int_{a'_{\min}}^{a'_{\max}} d\; f_D(d \mid i)\, f_I(i \mid a')\, f_{A'}^{MAX}(a';T)\, \mathrm{d}a'\, \mathrm{d}i\, \mathrm{d}d \\ &= \int_{i_{\min}}^{i_{\max}} \int_{a'_{\min}}^{a'_{\max}} E\left[D \mid i\right] f_I(i \mid a')\, f_{A'}^{MAX}(a';T)\, \mathrm{d}a'\, \mathrm{d}i\, \mathrm{d}d \end{aligned}$$

Where

$$E\left[D \mid i\right] = \int_{d_{\min}}^{d_{\max}} d\; f_D(d \mid i)\, \mathrm{d}d$$

When the mean expected damage for a given intensity is plotted against intensity we obtain a vulnerability curve. The conditional probability distribution functions are given in the form of a DPM. In ATC-13 there are seven damage states and seven MM intensity levels and by considering the central damage factors (CDF) we can replace the integral with a summation:

$$E\left[D \mid i\right] = \sum_{j=1}^{7} CDF_j \, DPM_{ij}$$

In the vulnerability curves that the PSRA produces, damage values for the MM intensity values in the range IV to VI are obtained by linear extrapolation since the derived central damage factors are not available for intensity levels less than VI. As stated previously, any intensity level less than IV implies zero damage.

Next, we need to define the remaining conditional probability distribution functions. For the intensity given PGA, we assume that intensity follows a Gaussian distribution:

$$f_I\left(i \mid a'\right) = \frac{1}{\sigma_I \sqrt{2\pi}} \exp\left\{ -\frac{\left(i - E\left[I \mid a'\right]\right)^2}{2\sigma_I^2} \right\}$$

where $E\left[I \mid a'\right] = 10.5 + 1.48 \ln a'$ (Trifunac and Brady, 1975) and $\sigma_I = 0.75$ (McGuire, 1993; Cao *et al*, 1999).

Finally, we have to specify the probability distribution function of the seismic hazard. Engineering seismologists usually assume that the occurrence of events with a PGA larger than the minimum PGA of engineering interest follows a Poisson distribution. The cumulative distribution of the largest PGA recorded at the site is given by:

$$F_{A'}^{MAX}\left(a';T\right) = \begin{cases} 0 & for \quad a' < a'_{\min} \\ \dfrac{\exp\left\{-\nu \mathrm{T}\left[1 - F_{A'}\left(a'\right)\right]\right\} - \exp\left(-\nu \mathrm{T}\right)}{1 - \exp\left(-\nu \mathrm{T}\right)} & for \quad a'_{\min} \le a' \le a'_{\max} \\ 1 & for \quad a' > a'_{\max} \end{cases}$$

Where $F_{A'}\left(a'\right)$ is the cumulative distribution of the PGA and follows the truncated Pareto distribution:

$$F_{A'}\left(a'\right) = \begin{cases} 0 & for \quad a' < a'_{\min} \\ \dfrac{a'^{-\gamma}_{\min} - a'^{\gamma}}{a'^{-\gamma}_{\min} - a'^{-\gamma}_{\max}} & for \quad a'_{\min} \le a' \le a'_{\max} \\ 1 & for \quad a' > a'_{\max} \end{cases}$$

It then follows that:

$$f_{A'}^{MAX}(a';T) = \nu T\ f_{A'}(a') F_{A'}^{MAX}(a';T) \frac{\exp\left\{-\nu \mathrm{T}\left[1-F_{A'}(a')\right]\right\}}{\exp\left\{-\nu \mathrm{T}\left[1-F_{A'}(a')\right]\right\} - \exp(-\nu \mathrm{T})}$$

Where ν and γ are parameters that are estimated according to the maximum likelihood procedure in the assessment.

In order to summarise the results of the PSRA effectively, some curves are examined. The basic seismic hazard curve combines the estimated distribution of the PGA and the relationship between the PGA and MM intensities. The estimated distribution of the PGA is derived by combining the information on seismic hazard with the information of the PGA with distance. Finally, seismic risk curves can be created detailing the annual probabilities of exceedance of given values of damage. This is done by combining the seismic hazard curve with the vulnerability curves.

4. Comparison of the parameter estimates for the South African case

4.1 Background

In order to compare the effect of the different estimators on insurance losses, a PSRA is conducted for the South African landscape. South Africa's seismic experience is characterised by relatively frequent small events (i.e. those smaller than magnitude 4) and very few large events. The largest seismic event in South Africa took place in the Ceres-Tulbagh region in 1969 which exhibited a magnitude of 6.7. (Davies and Kijko, 2003)

For the purposes of the study, we consider those events with magnitudes of 3.8 or more, since these are the seismic events which will most likely cause significant damage to insured buildings (Kijko and Smit, 2012). The largest possible earthquake was limited to a magnitude of 7, due to historical seismic activity in South Africa (Davies and Kijko, 2003). A catalogue detailing all the measurable seismic activity in South Africa between 1901 and 2013 was considered. The specific area under consideration was an area with the centre of Cape Town at its centre and a radius of 450km around this point, as illustrated in image 4.1.1. Notably, this area included the only nuclear power station in South Africa, and the Green Point Stadium which is shown in Figure 4.1.2.

In terms of uncertainty, we will assume that the magnitude observations have a standard deviation of approximately 30%, the b-parameter has a standard deviation of $\frac{b}{\sqrt{n}}$ and that the activity rate, λ, has a standard deviation of $\sqrt{\lambda}$, since it follows a Poisson distribution. The characteristics of the catalogue are summarised in Table 4.1.1 below (Kijko, 2011).

Figure 4.1.1

Map of the area under investigation in the PSRA conducted

(Source: AfriGIS (Pty) Ltd)

Figure 4.1.2

Image of Green Point Stadium in Cape Town, South Africa

(Source: www.woodford.co.za)

Three analyses are conducted in order to investigate the effects of uncertainty and the different methodologies for estimating β:

1. A sensitivity test with varying values of b, namely an assumed value of 1, and estimates of one standard deviation more, and one less than the assumed value.
2. A sensitivity test with varying values of the activity rate, namely the mean activity rate as estimated by evaluating the catalogue, as well as an activity rate of one standard deviation more than the mean rate and one less than the activity rate.
3. A side-by-side comparison of the effects of the b-values that are estimated by the different methodologies discussed in section 2 on elements of the PSRA. For the purposes of the methodology investigation, the estimators discussed in Section 2 are derived for the specific catalogue in question and the PSRA applied and compared. The results are summarised in Table 4.1.2.

The specific distribution of building classes for metropolitan areas in South Africa is outlined in Table 4.1.3. Note that four building classes, 3, 7, 8 and 9, make up the majority of the urban structures as mentioned in section 3.

Table 4.1.1

Characteristics of the earthquake catalogue

Characteristic	**Value**
Start date	1901
End date	2013
$m_{\min}$	3.8
$m_{\max}$	7.0
$\bar{m}$	4.2
Number of events larger than 4.0	1307
λ	12

Table 4.1.2

Estimates of the b-value using different methods on the same catalogue

Description	**Equation Number**	**b-value Estimate**
Aki-Utsu	2.3.1	1.0391
Double truncated exponential distributed magnitudes	2.3.5	1.0355
Double truncated exponential distributed magnitudes + Gaussian errors (σ=0.2)	2.4.1	1.0514
Double truncated exponential distributed magnitudes + Laplacian errors (σ=0.3)	2.4.2	1.0156

Table 4.1.3

Distribution of building class types in metropolitan areas in South Africa

Class	Class Description	Class distribution (% of total replacement costs)
1	Wood frame, low rise	0.09%
2	Light metal, low rise	0.10%
3	Unreinforced masonry, with load-bearing wall, low rise	9.17%
4	Unreinforced masonry, without load-bearing wall, low rise	0.09%
5	Unreinforced masonry, with load-bearing wall, medium rise	5.06%
6	Reinforced concrete shear wall, with moment resisting frame, medium rise	5.14%
7	Reinforced concrete shear wall, with moment resisting frame, high rise	13.80%
8	Reinforced concrete shear wall, without moment resisting frame, medium rise	17.48%
9	Reinforced concrete shear wall, without moment resisting frame, high rise	46.01%
10	Braced steel frame, low rise	0.79%
11	Precast concrete, low rise	0.51%
12	Long span, low rise	0.99%

(Source: Davies and Kijko, 2003)

4.2 Results

Investigation 1:

Three different permutations of the PSRA are conducted for values of b of 0.95, 1 and 1.05 compared to examine any notable differences. Graph 4.2.1 demonstrates the different distributions of the return period for a range of peak ground acceleration values. Graph 4.2.2 demonstrates the relationship between the weighted mean losses of the building classes, with weights as shown in table 4.1.3, against the levels of modified Mercalli intensity. Finally, Graph 4.2.3 demonstrates the probabilities of achieving certain levels of loss if the building classes are combined as in Table 4.1.3.

When considering graphs 4.2.1 and 4.2.2 in terms of insurance losses, we have to look at them in comparison. The graphs imply, and reiterate the intuitive assumption, that variation in the parameters related to the Gutenberg-Richter relation will only affect the peak ground acceleration values directly and will not influence how intensity will affect losses. This means that we know that the variation in losses associated with earthquakes in this particular study is due to changes in the parameters of the Gutenberg-Richter relation. Therefore we can draw no further inference about the differences from graph 4.2.2.

Some relevant arguments can be stated about graph 4.2.1 and the peak ground acceleration. As expected, a higher b value will lead to a quicker acceleration of the return period. Conversely, the lower b value implies a much slower acceleration of the return period in terms of peak ground acceleration. It is also notable that the maximum return period for a PGA of around 0.7g is much higher that for the models with higher b values. Notably, deviation of the three values for λ only occurs after a peak ground acceleration of 0.3g or even 0.4g has been reached.

Graph 4.2.1

Return periods for varying b-values

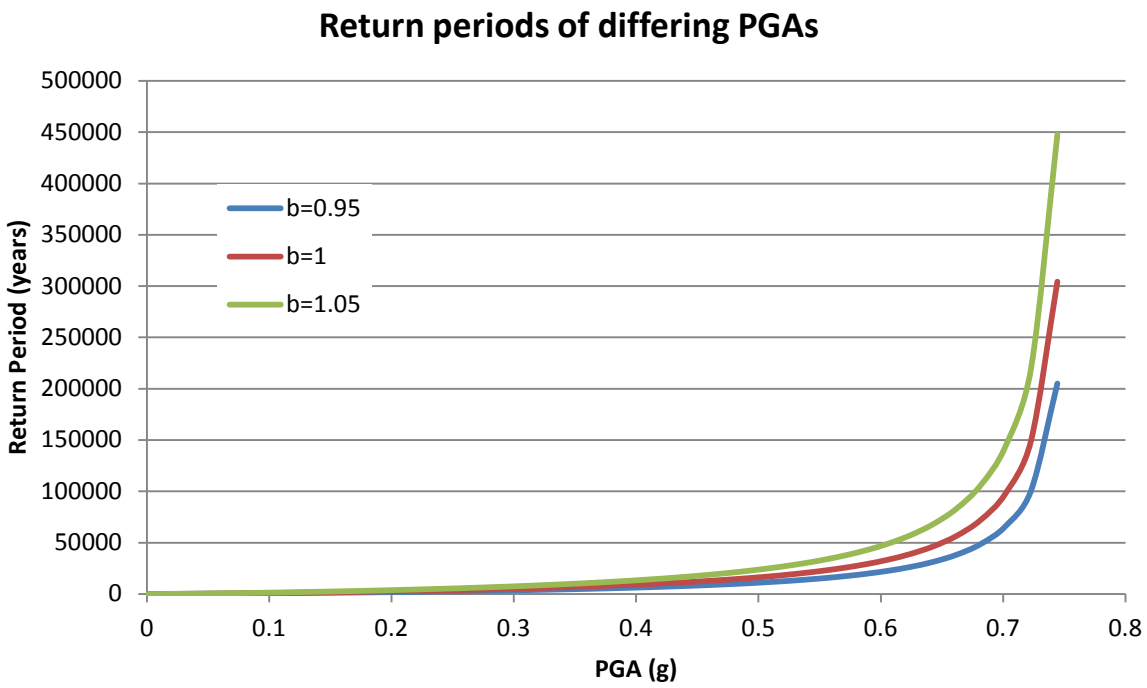

Graph 4.2.2

Comparison of mean damage per level of intensity

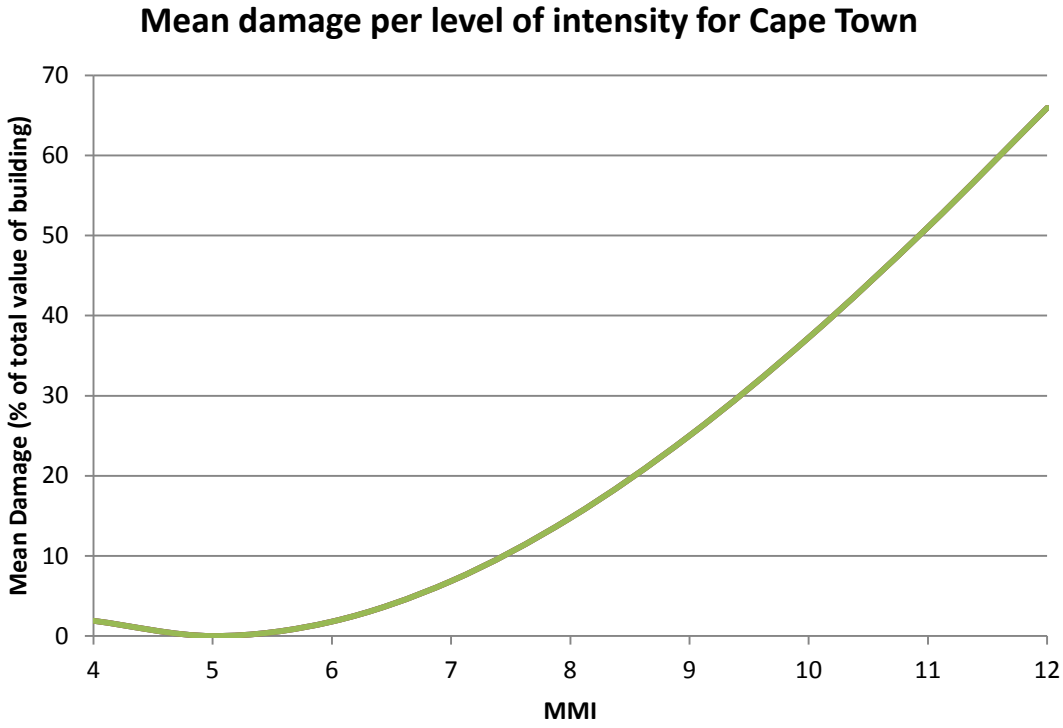

Graph 4.2.3

Comparison of mean losses for differing b-values

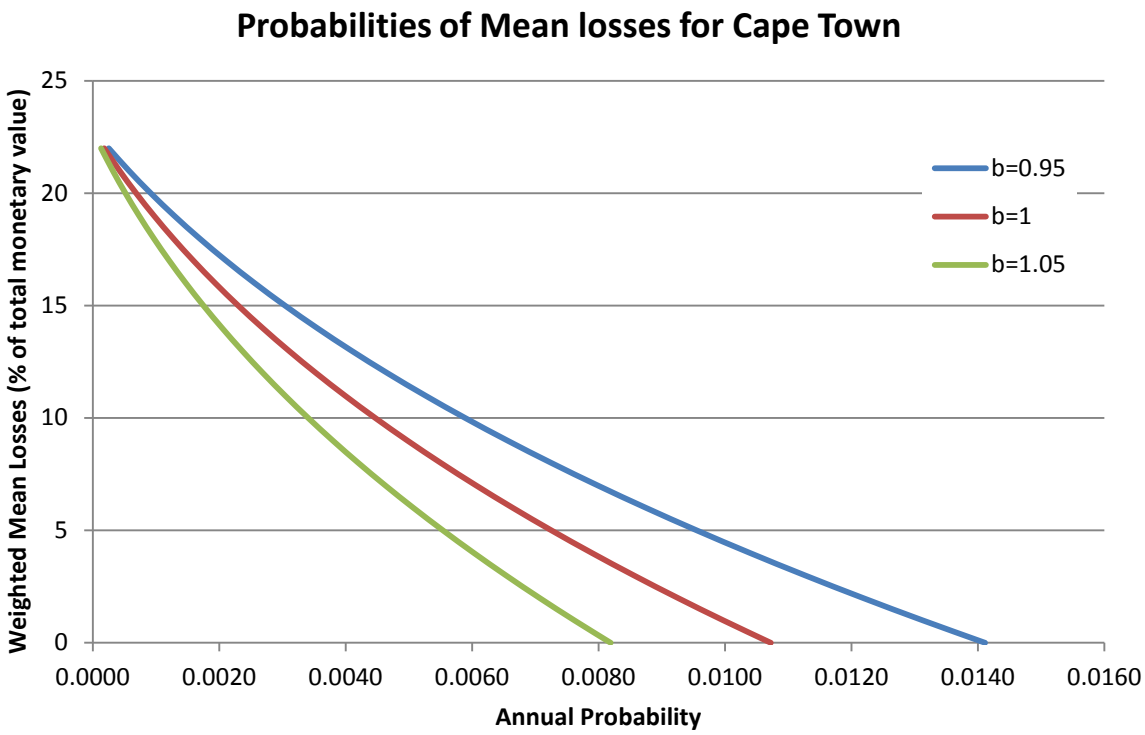

From consideration of graphs 4.2.1 and 4.2.2 we know that the variation in graph 4.2.3 is solely due to the effect of changes in the b-value on the peak ground acceleration. When considering individual building classes, the results look very similar to graph 4.2.3, therefore considering the mean damage is a good approximation of a well-balanced portfolio of insurance risks and small deviations from the mean distribution are negligible. The results depicted in graph 4.2.3 make intuitive sense.

Higher b values will lead to lower probabilities of damage since the ratios of small to large seismic events are larger. This implies that fewer large events will occur in relation to small events that are likely not to cause any real damage to structures. The converse argument holds for lower values of b. Variations in the b-value are once again compared to the benchmark *b* value of 1.

Investigation 2:

Three different permutations of the PSRA are conducted for values of λ of 3, 5 and 7 and compared to examine any notable differences. The lower value for the activity rate was specified as 1, since it is assumed that an activity rate of less than 1 for earthquakes of magnitude 5 or higher for the area under investigation can be approximated to 1. Graph 4.2.4 demonstrates the different distributions of the return period for a range of peak ground acceleration values.

A graph demonstrating the relationship between the weighted mean losses of the building classes, with weights as shown in table 4.1.3, against the levels of modified Mercalli intensity is not included again. For reference Graph 4.2.2 can be used and all arguments about influence of parameters follow from the interpretation of Investigation 1. Graph 4.2.5 demonstrates the probabilities of

achieving certain levels of loss if the building classes are combined as in Table 4.1.3. Note that in the legends of both graph 4.2.4 and 4.2.5, $la = \lambda$.

Graph 4.2.4

Return periods for differing activity rates

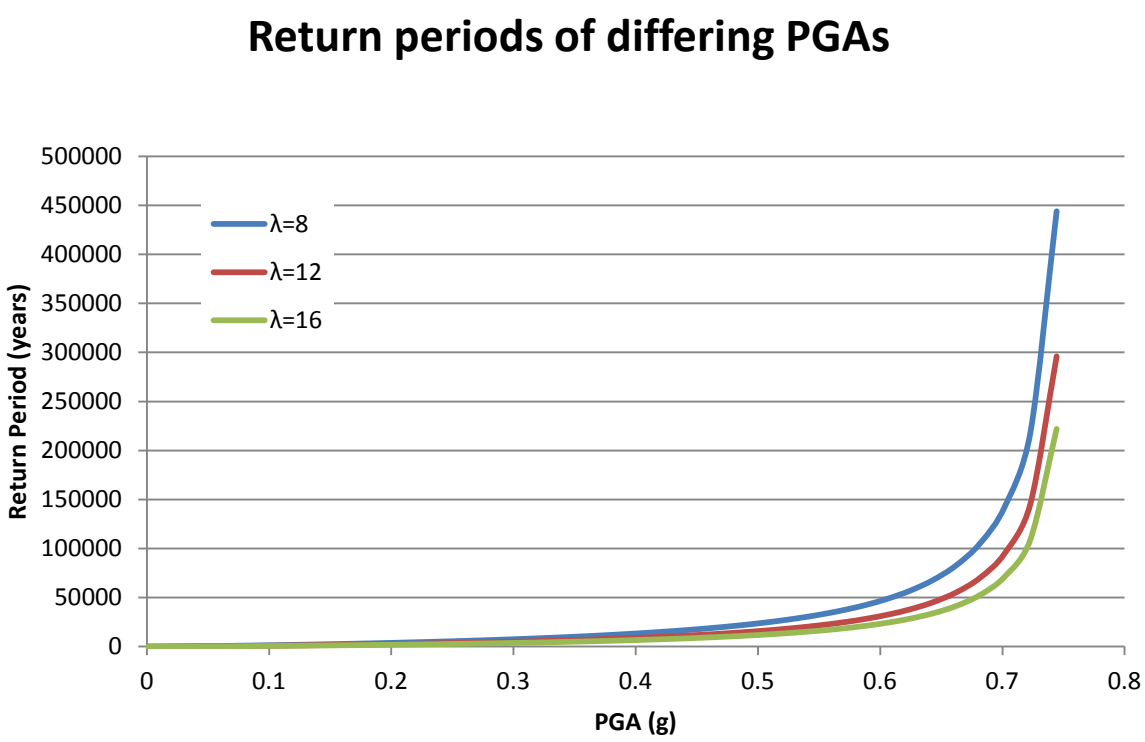

The relationships depicted in graph 4.2.4 are consistent with our understanding of the effects of the activity rate or λ. The mean activity rate for seismic events of magnitude 3.8 or higher is calculated as 12 and has been used as the benchmark. Lower values of λ will imply a faster acceleration of the return period for lower peak ground acceleration values. The peak ground acceleration will also be lower than or equal to that of lower values but with a higher return period. This relationship implies that lower values of λ imply less seismic activity which is exactly the case.

Conversely, a higher value of λ implies that earthquake activity is increased since peak ground acceleration is higher for lower return periods although acceleration is not as quick. Notably, deviation of the three values for λ only occurs after a peak ground acceleration of 0.1g has been reached.

From consideration of graphs 4.2.4 and 4.2.2 we know that the variation in graph 4.2.5 is solely due to the effect of changes in the b-value on the peak ground acceleration. Once again, when considering individual building classes, the results look very similar to graph 4.2.5, therefore considering the mean damage is a good approximation of a well-balanced portfolio of insurance risks and small deviations from the mean distribution will be negligible.

The results depicted in graph 4.2.5 make intuitive sense. Higher activity rates will lead to higher probabilities of loss since more earthquakes above magnitude 3.8 are expected to happen within a single year. The converse argument for lower activity rates holds. Variations in the activity rate are

once again compared to the benchmark value of 12. The variation in the probabilities is similar than that of graph 4.2.3.

Graph 4.2.5

Comparison of mean losses for differing activity rates

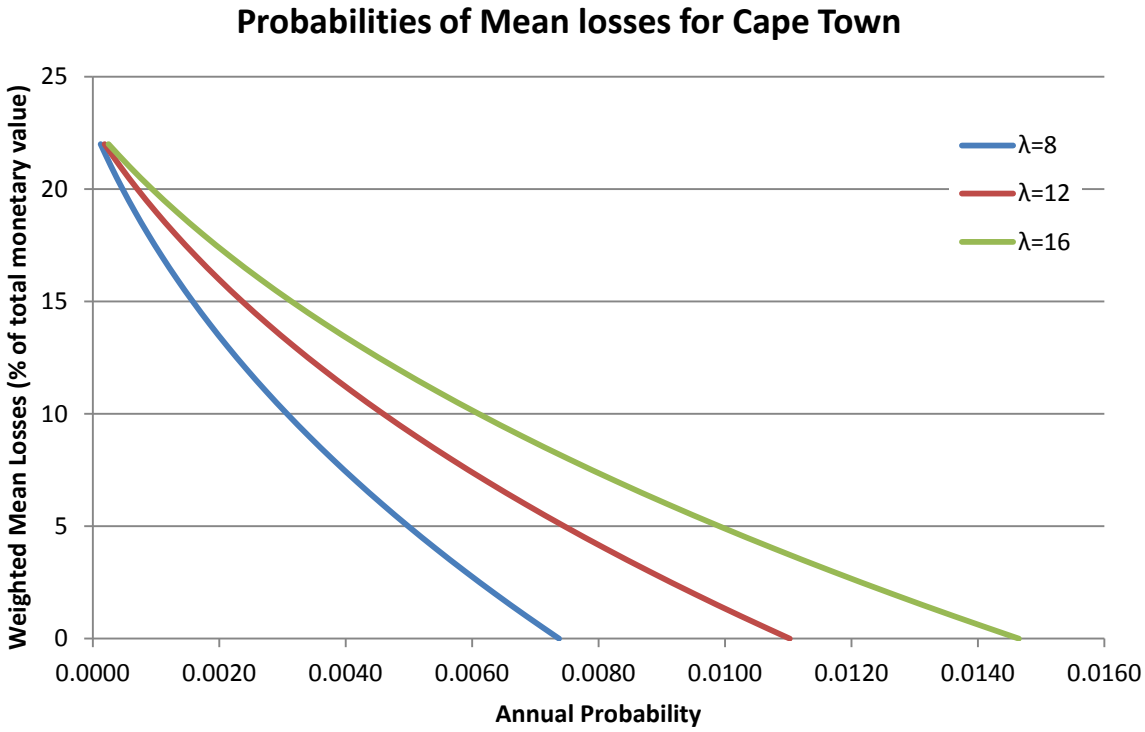

Investigation 3:

Four different permutations of the PSRA are conducted for values of b as outlined in table 4.1.2 compared to examine any notable differences. Graph 4.2.6 demonstrates the different distributions of the return period for a range of peak ground acceleration values. A graph demonstrating the relationship between the weighted mean losses of the building classes, with weights as shown in table 4.1.3, against the levels of modified Mercalli intensity is not included again. For reference Graph 4.2.2 can be used and all arguments about influence of parameters follow from the interpretation of Investigation 1. Graph 4.2.7 demonstrates the probabilities of achieving certain levels of loss if the building classes are combined as in Table 4.1.3.

In keeping with the results from Investigation 1, higher b values yield lower probabilities of mean losses and higher b-values yield higher probabilities of mean losses. The classic and bounded classic estimates yield results that are very similar. This is expected since their values are close to one another and they are based on similar methodologies. The results show that the estimator which includes Laplacian error has the shortest return periods for given levels of peak ground acceleration. The peak ground acceleration for the estimator that includes Gaussian errors has the highest return period. The differences, however, are not very significant since there is little difference between these return periods.

Graph 4.2.6

Return periods for different estimates of the b-value

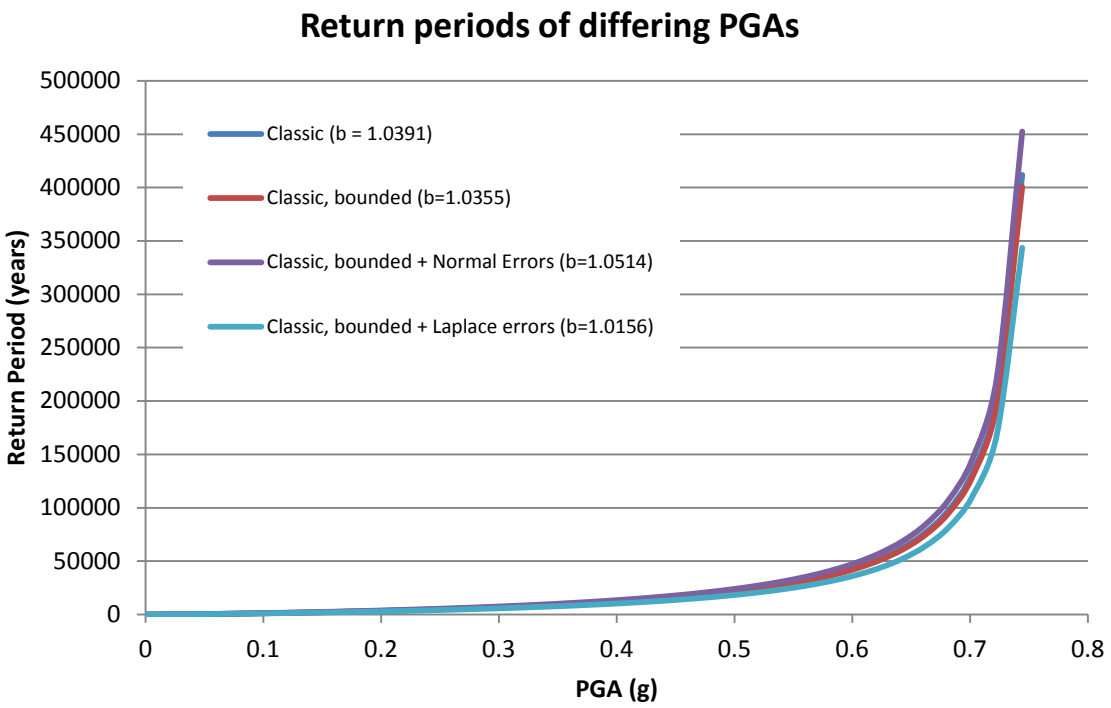

Graph 4.2.7

Comparison of mean losses for different estimates of the b-value

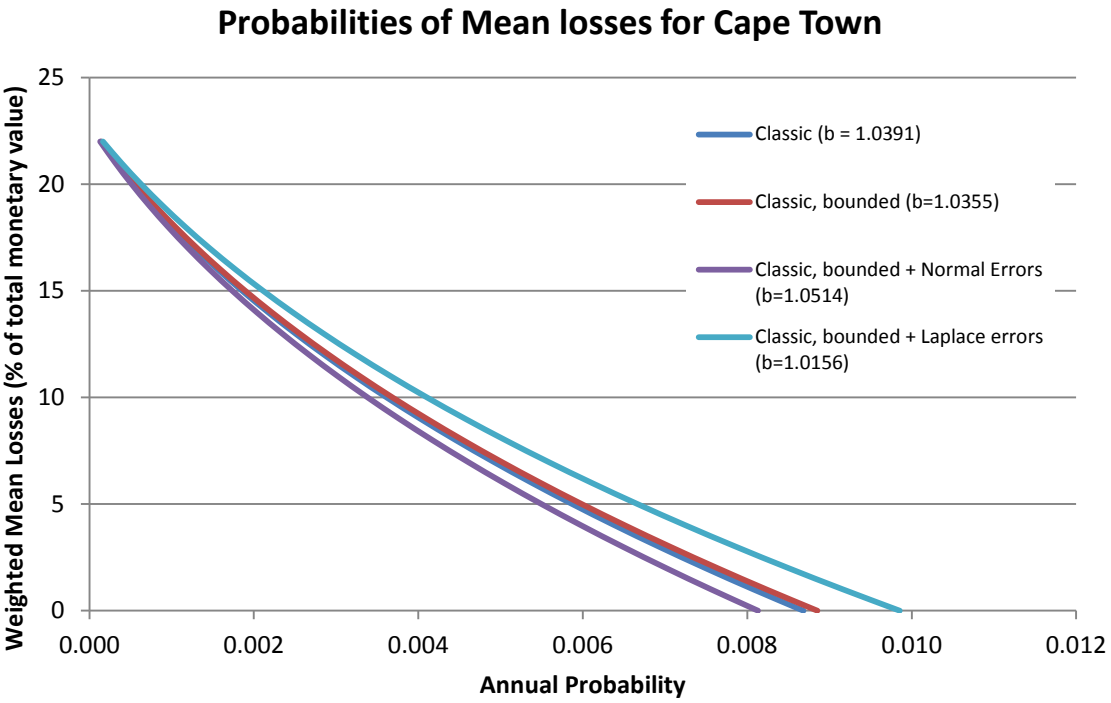

Interestingly, the estimator that includes Gaussian error is slightly higher than those estimates that do not include errors. The estimates that yield results in the middle of the possible loss distributions are the classical and bounded classical estimates. This is expected since their values are very close to one another. This could mean that there is an argument to be made that the classic estimator continues to be a good approximation of the underlying b-value contained in earthquake catalogues. However, it is no great exercise to expand the estimate to include the maximum possible earthquake within the region under consideration.

The relationship of the classic estimate with other estimates could imply that the classic estimate is a reasonable estimator for areas of low seismicity, but this is largely dependent on the underlying assumptions and the data, such as the minimum and maximum earthquake values considered.

It must also be noted that the choice of method of estimation for the b-value is largely a function of the quality of the data. For catalogues where little information is available about their origin and composition, the classic (Aki-Utsu) estimator would be a good place to start. For catalogues that consist of information from a single source, and are fairly recent, the bounded classical estimator will be a reasonable choice. When catalogues are compiled using several data sources, averaging occurs over the different data points. In these cases, the bounded classical estimator that includes Gaussian errors will be a good choice of method. The additional assumption that observation errors are fairly small, for example a standard deviation from the mean of 0.1 to 0.2 units of magnitude, will be reasonable. Finally, for catalogues with large probable outliers, in particular historic catalogues, the bounded classical estimator which included Laplace errors will be a good method to employ. The reasonable assumption in such cases is that the observation errors are fairly large, *i.e.* that the standard deviation of these errors lies around 0.3 units of magnitude for each observation.

5. Conclusion

While subjective to some degree, the PSRA is a good way of testing the potential losses related to seismic events for a particular area. The investigations conducted indicate that variability in the parameters of the Gutenberg-Richter relation influence the probabilities of potential mean losses from seismic activity. Furthermore, the investigations indicate that, for areas of weak seismicity, changes in the parameters have significant effects on loss probabilities.

It can clearly be seen from the results of the investigations that lower estimates of the b-value and higher estimates of the activity rate lead to over-cautious loss estimates. Similarly, higher estimates of the b-value and lower estimates of the activity rate, lead to under-cautious loss estimates.

Different methodologies for estimating the b-value yield vastly different results, in particular for areas of weak seismicity, but it is vitally important to consider the nature of the catalogue when deciding on the best estimate to use. It may be a good idea to include a possible range of estimates for the parameters of the Gutenberg-Richter relation in order to draw more accurate inferences about the potential losses.

Further investigation for a number of catalogues will most likely yield more meaningful ideas about which methodology will most accurately estimate the b-value. The sensitivity of loss probabilities will most likely be less severe for areas of high seismicity with less scarce data and further investigation is required.

Appendix 1:

Most destructive earthquakes, in terms of number of deaths

Date UTC	Location	Deaths	Magnitude
856/12/22	Iran, Damghan	200000	
893/03/23	Iran, Ardabil	150000	
1138/08/09	Syria, Aleppo	230000	
1268	Asia Minor, Silicia	60000	
1290/09/27	China, Chihli	100000	
1556/01/23	Shaanxi (Shensi), China	830000	8
1667/11/	Caucasia, Shemakha	80000	
1693/01/11	Italy, Sicily	60000	7.5
1727/11/18	Iran, Tabriz	77000	
1755/11/01	Portugal, Lisbon	70000	8.7
1783/02/04	Italy, Calabria	50000	
1908/12/28	Messina, Italy	72000	7.2
1920/12/16	Haiyuan, Ningxia (Ning-hsia), China	200000	7.8
1923/09/01	Kanto (Kwanto), Japan	142800	7.9
1948/10/05	Ashgabat (Ashkhabad), Turkmenistan (Turkmeniya, USSR)	110000	7.3
1970/05/31	Chimbote, Peru	70000	7.9
1976/07/27	Tangshan, China	242769	7.5
1990/06/20	Western Iran	50000	7.4
2004/12/26	Sumatra	227898	9.1
2005/10/08	Pakistan	86000	7.6
2008/05/12	Eastern Sichuan, China	87587	7.9
2010/01/12	Haiti region	316000	7.0

Source: U.S. Geological Survey, 2012

Appendix 2:

A summary of the Modified Mercalli Intensity scale:

I. Not felt except by a very few under especially favourable conditions.

II. Felt only by a few persons at rest, especially on upper floors of buildings.

III. Felt quite noticeably by persons indoors, especially on upper floors of buildings. Many people do not recognize it as an earthquake. Parked motor cars may rock slightly. Vibrations similar to the passing of a truck. Duration estimated.

IV. Felt indoors by many, outdoors by few during the day. At night, some woke up. Dishes, windows, doors disturbed; walls make cracking sound. Sensation like heavy truck striking building. Parked motor cars rocked noticeably.

V. Felt by nearly everyone; many woke up. Some dishes, windows broken. Unstable objects overturned. Pendulum clocks may stop.

VI. Felt by all, many frightened. Some heavy furniture moved; a few instances of fallen plaster. Damage slight.

VII. Damage negligible in buildings of good design and construction; slight to moderate in well-built ordinary structures; considerable damage in poorly built or badly designed structures; some chimneys broken.

VIII. Damage slight in specially designed structures; considerable damage in ordinary substantial buildings with partial collapse. Damage great in poorly built structures. Fall of chimneys, factory stacks, columns, monuments, walls. Heavy furniture overturned.

IX. Damage considerable in specially designed structures; well-designed frame structures thrown out of plumb. Damage great in substantial buildings, with partial collapse. Buildings shifted off foundations.

X. Some well-built wooden structures destroyed; most masonry and frame structures destroyed with foundations. Rails bent.

XI. Few, if any (masonry) structures remain standing. Bridges destroyed. Rails bent extensively.

XII. Damage total. Lines of sight and level are distorted. Objects thrown into the air.

Source: US Geological Survey, 1989

References

AfriGIS (Pty) Ltd 2014, 10/03/2014 - last update, Available: http://maps.google.co.za [2014/03/10]

Aki, K. 1965, "Maximum Likelihood Estimate of b in the formula logN=a-bm and its Confidence Limits", Bulletin of the Earthquake Research Institute, vol. 43, pp. 273--279.

Ambraseys, N. 1995, "The prediction of earthquake peak ground acceleration in Europe", Earthquake Engineering & Structural Dynamics, vol. 24, no. 4, pp. 467-490.

AngloGold Ashanti, 2012. West Wits Country Report 2012. Johannesburg, 2012.

ATC-13, Applied Technology Council 1985, "ATC 13: Earthquake Damage Evaluation Data for California", Federal Emergency Management Agency Redwood City, CA.

Ayele, A. & Kulhánek, O. 1997, "Spatial and temporal variations of seismicity in the Horn of Africa from 1960 to 1993", Geophysical Journal International, vol. 130, no. 3, pp. 805-810.

Bender, F. & Bannert, D.N. 1983, Geology of Burma, Gebr. Borntraeger.

Bengoubou-Valérius, M. & Gibert, D. 2013, "Bootstrap determination of the reliability of b-values: an assessment of statistical estimators with synthetic magnitude series", Natural Hazards, vol. 65, no. 1, pp. 443-459.

Boore, D.M. & Joyner, W.B. 1982, "The empirical prediction of ground motion", *Bulletin of the Seismological Society of America,* vol. 72, no. 6B, pp. S43-S60.

Cao, T., Petersen, M.D., Cramer, C.H., Toppozada, T.R., Reichle, M.S. & Davis, J.F. 1999, "The calculation of expected loss using probabilistic seismic hazard", *Bulletin of the Seismological Society of America,* vol. 89, no. 4, pp. 867-876.

Cornell, C.A. 1968, "Engineering seismic risk analysis", Bulletin of the Seismological Society of America, vol. 58, no. 5, pp. 1583-1606.

Davies, N. and Kijko, A. 2003, “Seismic Risk Assessment: with an application to the South African Insurance Industry”, South African Actuarial Journal, vol. 3, pp. 1-28.

Dowrick, D. & Rhoades, D. 2000, "Earthquake damage and risk experience and modeling in New Zealand", Proceedings of the 12th world conference on earthquake engineering, Auckland.

EMS, 1998, European Seismological Commission 1998, "European Macroseismic Scale 1998", *European Center of Geodynamics and Seismology*.

Engelhardt, B. & Bain, L. 1992, "Introduction to probability and mathematical statistics", PWS-KENT Publishing Company.

Gerstenberger, M., Wiemer, S. & Giardini, D. 2001, "A systematic test of the hypothesis that the b value varies with depth in California", Geophysical Research Letters, vol. 28, no. 1, pp. 57-60.

Grossi, P. & Kunreuther, H. 2005, Catastrophe modeling: A new approach to managing risk, Springer.

Grossi, P. & Zoback, M. 2009, Catastrophe Modeling and California Earthquake Risk: A 20-year perspective, Risk Management Solutions, www.rms.com.

Gutenberg, B.R. "CF (1954)", Seismicity of the earth and associated phenomena, .

Kagan, Y. 1999, "Universality of the seismic moment-frequency relation" in Seismicity Patterns, their Statistical Significance and Physical Meaning Springer, pp. 537-573.

Kijko, A. 1988, "Maximum likelihood estimation of Gutenberg-Richter b parameter for uncertain magnitude values", Pure and Applied Geophysics, vol. 127, no. 4, pp. 573-579.

Kijko, A. 2011, "Seismic Hazard" in *Encyclopedia of Solid Earth Geophysics*, Encyclopedia of Earth Sciences Series, Springer, pp. 1107-1121.

Kijko, A. & Smit, A. 2012, "Extension of the Aki-Utsu b-Value Estimator for Incomplete Catalogs", Bulletin of the Seismological Society of America, vol. 102, no. 3, pp. 1283-1287.

Kijko, A. & Smit, A. 2012, *Probabilistic Seismic Hazard and Risk Assessment for the eThikweni Municipality*, Aon Re Africa (Pty) Limited T/A Aon Benfield, Pretoria, South Africa.

Ku, H. 1969, "Notes on the use of propagation of error formulas", Precision Measurement and Calibration, NBS SP 3D0, vol. 1, pp. 331-341.

Liechti, D., Ruettener, E., Eugster, S. & Streit, R. 2000, "The impact of a and b value uncertainty on loss estimation in the reinsurance industry".

Marzocchi, W. & Sandri, L. 2003, "A review and new insights on the estimation of the b-value and its uncertainty", Annals of geophysics, .

Page, R. 1968, "Focal depths of aftershocks", Journal of Geophysical Research, vol. 73, no. 12, pp. 3897-3903.

Paine, C. 2004, Reinsurance, Institute of Financial Services.

panoramio.com 2008, 25/10/2008 - last update, ***University of Pretoria, HSB***. Available: *http://www.panoramio.com/photo/15322275* [2012/12/10]

Rhoades, D. 1996, "Estimation of the Gutenberg-Richter relation allowing for individual earthquake magnitude uncertainties", Tectonophysics, vol. 258, no. 1, pp. 71-83.

Richter, C.F. 1935, "An instrumental earthquake magnitude scale", Bull.Seism.Soc.Am, vol. 25, no. 1, pp. 1-32.

Sandri, L. & Marzocchi, W. 2006, "A technical note on the bias in the estimation of the b-value and its uncertainty through the least squares technique".

Schmid, E. & Schaad, W. 1995, "A database for worldwide seismicity quantification", Natural Hazards, vol. 12, no. 2, pp. 153-160.

Schorlemmer, D., Neri, G., Wiemer, S. & Mostaccio, A. 2003, "Stability and significance tests for b-value anomalies: Example from the Tyrrhenian Sea", Geophysical Research Letters, vol. 30, no. 16.

Senior Seismic Hazard Analysis Committee (SSHAC), Budnitz, R.J., US Nuclear Regulatory Commission. Office of Nuclear Regulatory Research. Division of Engineering Technology, Lawrence Livermore National Laboratory, United States. Dept. of Energy & Electric Power Research Institute 1997, Recommendations for probabilistic seismic hazard analysis: guidance on uncertainty and use of experts, US Nuclear Regulatory Commission.

Shah, H., Boyle, R. & Dong, W. 1991, "Geographic information systems and artificial intelligence: an application for seismic zonation", Proceeding of the Fourth International Conference on Seismic Zonation, pp. 487.

Shi, Y. & Bolt, B.A. 1982, "The standard error of the magnitude-frequency b value", Bulletin of the Seismological Society of America, vol. 72, no. 5, pp. 1677-1687.

Tinti, S. & Mulargia, F. 1985, "Effects of magnitude uncertainties on estimating the parameters in the Gutenberg-Richter frequency-magnitude law", Bulletin of the Seismological Society of America, vol. 75, no. 6, pp. 1681-1697.

Trifunac, M.D. & Brady, A.G. 1975, "A study on the duration of strong earthquake ground motion", *Bulletin of the Seismological Society of America,* vol. 65, no. 3, pp. 581-626.

U.S, Geological Survey, 1989, *The Severity of an Earthquake*, U. S. Geological Survey General Interest Publication, U.S. GOVERNMENT PRINTING OFFICE: 1989-288-913.

U.S. Geological Survey 2008, 03/12/2012 - last update*, **Earthquakes with 50,000 or more deaths,*** Available: *http://earthquake.usgs.gov/earthquakes/world/most_destructive.php* [2013/12/10]

Utsu, T. 1965, "A method for determining the value of b in a formula log n= a-bM showing the magnitude-frequency relation for earthquakes", Geophys.Bull.Hokkaido Univ, vol. 13, pp. 99-103.

Werner, M.J. & Sornette, D. 2008, "Magnitude uncertainties impact seismic rate estimates, forecasts, and predictability experiments", Journal of Geophysical Research: Solid Earth (1978–2012), vol. 113, no. B8.

Whitman, R.V., Reed, J.W. & Hong, S. 1973, "Earthquake damage probability matrices", Proceedings of the Fifth World conference on earthquake engineering, Rome, Italy: Palazzo Dei Congresi, , pp. 2540.

Wiemer, S. & Benoit, J.P. 1996, "Mapping the B-value anomaly at 100 km depth in the Alaska and New Zealand Subduction Zones", Geophysical Research Letters, vol. 23, no. 13, pp. 1557-1560.

Wiemer, S., McNutt, S.R. & Wyss, M. 1998, "Temporal and three-dimensional spatial analyses of the frequency–magnitude distribution near Long Valley Caldera, California", Geophysical Journal International, vol. 134, no. 2, pp. 409-421.

www.woodford.co.za 2014 - last update*, **Cape Town Photo 1,*** Available: *http://www.woodford.co.za/news/cape-town-photo1.jpg* [2014/03/10]